Supporting Information

Syntheses, Structures and Efficient Visible Light Driven Photocatalytic Properties of Layered Cuprous Halides Based on Two Types of Building Units

Ai-Huan Sun,[a] Qi Wei,[a] Ai-Ping Fu,[b] Song-De Han,[a] Jin-Hua Li[a] and Guo-Ming Wang*,[a]

[a]*College of Chemistry and Chemical Engineering, Qingdao University, Shandong 266071, P. R. China*

[b]*Laboratory of New Fiber Materials and Modern Textile, the Growing Base for State Key Laboratory, Qingdao University, Shandong 266071, P. R. China*

Table S1. Selected bond lengths (Å) for compounds **1-3**.

Compound 1			
Cu(1)-I(1)	2.5259(12)	Cu(3)-I(6)	2.6590(11)
Cu(1)-I(2)	2.5373(12)	Cu(3)-I(5)	2.6706(12)
Cu(1)-I(5)#1	2.5029(12)	Cu(4)-I(6)	2.5065(12)
Cu(2)-I(2)	2.7820(14)	Cu(4)-I(7)	2.5718(13)
Cu(2)-I(3)	2.6057(12)	Cu(4)-I(8)	2.6230(12)
Cu(2)-I(4)	2.6754(12)	Cu(5)-I(1)#2	2.6122(12)
Cu(2)-I(4)#1	2.6154(12)	Cu(5)-I(8)	2.6644(12)
Cu(3)-I(3)	2.6127(11)	Cu(5)-I(7)	2.6691(12)
Cu(3)-I(4)	2.6272(12)	Cu(5)-I(2)#2	2.6878(12)
Compound 2			
Cu(1)-I(1)	2.6455(15)	Cu(3)-I(8)	2.6708(15)
Cu(1)-I(4)	2.6494(15)	Cu(3)-I(5)	2.6808(15)
Cu(1)-I(2)	2.6607(15)	Cu(4)-I(7)	2.5944(15)
Cu(1)-I(3)	2.7026(15)	Cu(4)-I(6)#1	2.6123(16)
Cu(2)-I(5)	2.5133(14)	Cu(4)-I(6)	2.6667(16)
Cu(2)-I(3)	2.5381(14)	Cu(4)-I(3)#1	2.8465(18)
Cu(2)-I(4)	2.5697(15)	Cu(5)-I(8)	2.5062(16)
Cu(3)-I(7)	2.6205(15)	Cu(5)-I(1)#2	2.5639(16)
Cu(3)-I(6)	2.6316(14)	Cu(5)-I(2)#2	2.6139(15)
Compound 3			
Cu(1)-Br(1)	2.348(2)	Cu(3)-Br(6)	2.4021(16)
Cu(1)-Br(2)	2.503(3)	Cu(4)-Br(2)	2.679(2)
Cu(1)-Br(8)#2	2.401(2)	Cu(4)-Br(2)#1	2.5413(19)
Cu(2)-Br(1)	2.5033(16)	Cu(4)-Br(3)#1	2.4154(16)
Cu(2)-Br(2)	2.6373(16)	Cu(4)-Br(5)	2.4100(17)
Cu(2)-Br(3)	2.4326(16)	Cu(5)-Br(6)	2.4260(17)
Cu(2)-Br(4)	2.4194(15)	Cu(5)-Br(7)	2.3151(16)
Cu(3)-Br(4)	2.3584(17)	Cu(5)-Br(8)	2.4330(18)
Cu(3)-Br(5)	2.3483(16)		

Symmetry codes: For **1**: (#1) -*x*+1,-*y*+1,-*z*; (#2) -*x*+1/2,*y*+1/2,-*z*+1/2. For **2**: (#1) -*x*,-*y*,-*z*; (#2) *x*+1/2,-*y*+1/2,*z*-1/2. For **3**: (#1) -*x*+1,-*y*,-*z*; (#2) *x*-1/2,-*y*+1/2,*z*+1/2.

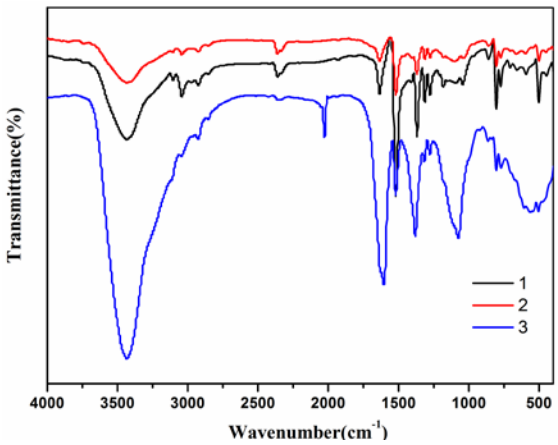

Figure S1. IR spectra of compounds **1**-**3**.

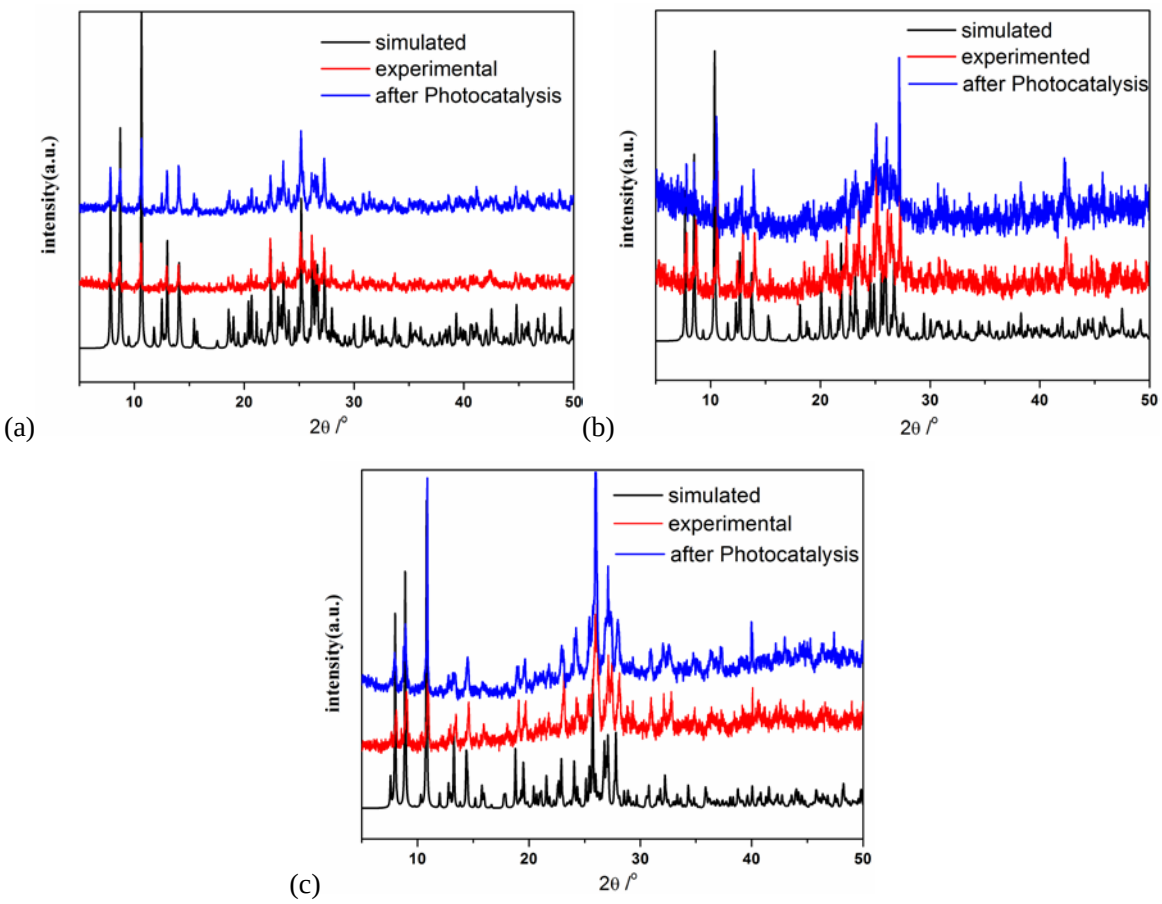

Figure S2. Experimental and simulated PXRD patterns of compounds **1** (a), **2** (b) and **3** (c).

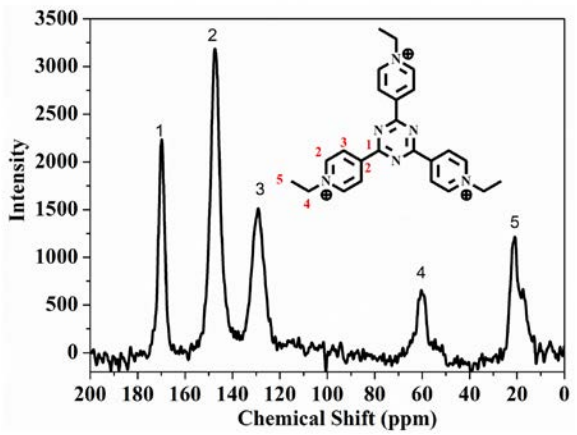

Figure S3. The solid ^{13}C NMR spectroscopy of compound **2**.

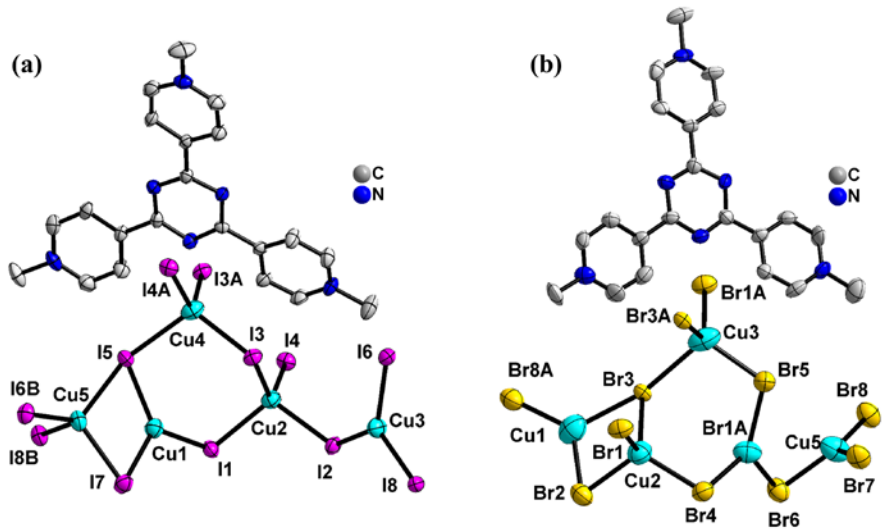

Figure S4 The asymmetric units and the coordination environment of Cu atoms of **1** (a) and of **3** (b). Symmetry operation for **1**: (A) 1−*x*, -1−*y*, −*z*; (B) -1+*x*, -1.5−*y*, -0.5+*z*. Symmetry operation for **3**: (A) 1−*x*, −*y*, −*z*; (B) 0.5+*x*, 0.5−*y*, -0.5+*z*.

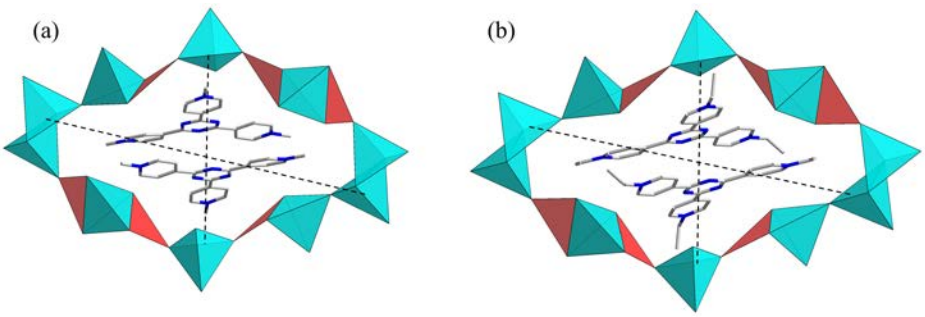

Figure S5. (a) View of the 16-MR window in **1** with the diameter of ~13.7×23.5 Å^2. (b) View of the 16-MR window in **2** with the diameter of ~14.0×23.7 Å^2. $[Et_3TPT]^{3+}$ in **2** is larger than the $[Me_3TPT]^{3+}$ in **1** in size, which results in larger windows in the layer of **2**.

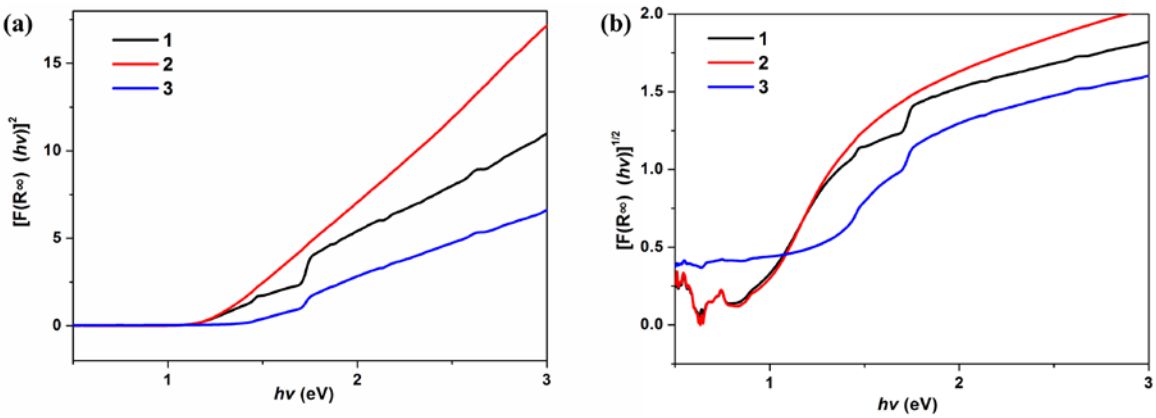

Figure S6. The band gap obtained from optical spectra. ((a) is [F(R∞) *hv*]^2 versus *hv*, and (b) is [F(R∞) (*hv*)]$^{1/2}$ versus *hv*).

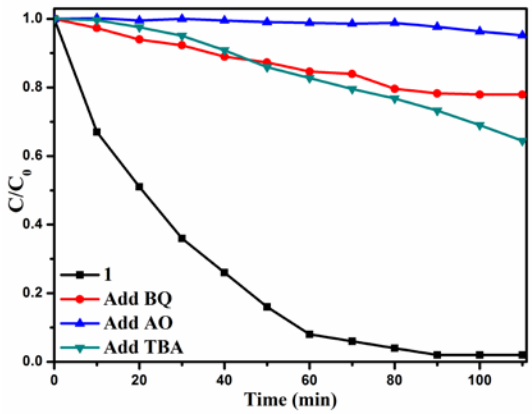

Figure S7. The effects of different scavengers (BQ: benzoquinone, AO: ammonium oxalate, TBA: *tert*-butyl alcohol) on MO under visible-light irradiation.

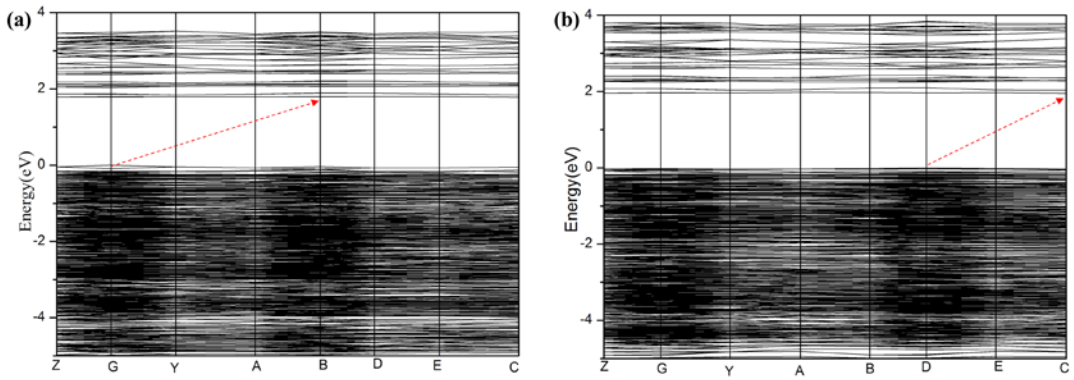

Figure S8. Band structures of compounds **1** (a) and **3** (b).

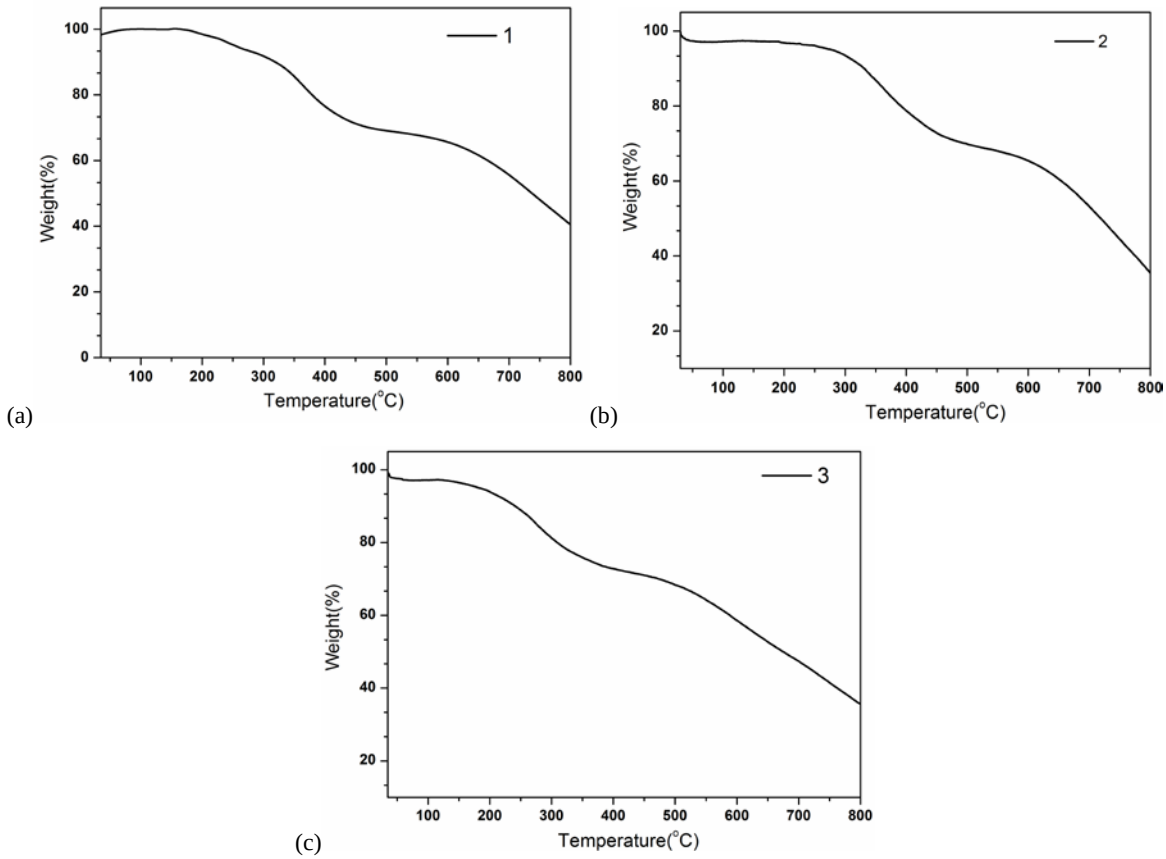

Figure S9. TG curves of compounds **1** (a), **2** (b) and **3** (c).